Investigation of the mixed alkali effect in boro-tellurite glasses – the role of NBO–BO switching in ion transport

M. Harish Bhat, Munia Ganguli and K. J. Rao*

Solid State and Structural Chemistry Unit, Indian Institute of Science, Bangalore 560 012, India

Glasses of the composition $30(Li,Na)_2O{\cdot}xB_2O_3{\cdot}(70–x)TeO_2$ ($20 \le x \le 50$) have been prepared using the melt-quenching method. Properties of these glasses have been measured and examined for the presence of mixed alkali effect (MAE). Infrared, Raman and ^{11}B HR MAS NMR spectroscopies have been used to investigate the structure of these glasses. DC and a.c. conductivities and dielectric properties have been measured over a wide range of frequencies and temperatures. Densities, molar volumes, glass transition temperatures, thermodynamic fragilities, infrared absorption frequencies, d.c. conductivities and activations barriers have been found to exhibit MAE. However, MAE does not manifest in the a.c. transport and dielectric relaxation parameters. Structure and bonding considerations account for the observed MAE in several properties. But the presence of MAE in d.c. conductivities and its absence in a.c. transport and dielectric phenomena is notable and its understanding requires a critical review of currently used conceptual basis of ion transport in oxide glasses. A new approach is therefore proposed in which the primary event in ion transport is the motion of negative charge through the non-bridging oxygen (NBO)–bridging oxygen (BO) switching. NBO–BO switching initiates the jump of alkali ions as the latter become energetically unstable in their positions. The present mechanism leaves unaffected the Arrhenius behaviour of d.c. conductivity, but with a new meaning of the parameters in it.

IT has been observed quite generally in alkali modified network oxide glasses, that the substitution of one alkali by another at a total fixed concentration of the alkalies gives rise to nonlinear variation of properties. This is most notable in properties related to alkali ion transport. The phenomenon is described as mixed alkali effect (MAE) and the subject has been reviewed and discussed extensively in the literature[1–4]. A number of models and theories have been proposed to account for MAE. Structural theories focus attention on efficient packing of space when dissimilar alkali ions are present in the glass than when only a single alkali is present. This causes an increase in the effective barrier for alkali ion motion. The other aspect is the blocking effect, where motion of one alkali ion is prevented by the other in its pathway[5,6]. Computer simulation studies suggest that alkali ions occupy preferred sites and peruse only such sites for their motion. Thus they define for themselves preferred pathways which are interrupted by the presence of dissimilar alkali ions in mixed alkali glasses[7,8]. In another elegant approach, stabilization of alkali ions in their own sites in the glass structure is considered as responsible for MAE. The stabilization is attributed to electrodynamic interactions between dipoles associated with dissimilar alkali ions oscillating in their own voronoi polyhedra[9]. There have also been suggestions of pairing of dissimilar alkali neighbours, which tends to immobilize both of them. Such pairing manifests as minimum in conductivity in mixed alkali compositions[10]. Another such approach has been the so-called interchange transport mechanism, according to which alkali ions in mixed alkali silicate glasses interchange their positions with respect to a nearby silicon and give rise to reduced conductivity in mixed alkali compositions[11,12]. Presence of MAE in (logarithmic) viscosity, $\ln(\eta)$, isokoms, viscosity activation barriers, E_η, kinetic fragilities, $F_{1/2}$ (estimated using viscosity data), d.c. conductivities, $\sigma_{d.c.}$, dielectric constants, ε', dielectric losses, $\tan\delta$, etc. has been reported in the literature and generally has been attributed to features like the rearrangement of constituent units in glass (melt) structure, higher negative enthalpy of mixing and greater correlation lengths[13–15] in ion motion. But detailed studies have shown that the mechanism of viscous flow remains unaffected in mixed alkali and single alkali borate glasses, and therefore the fragilities should remain unaffected in the mixed alkali compositions[16]. MAE in borate glasses is believed to be a structural effect associated with change in intermediate range order caused by the difference in cationic field strengths[17–19]. Approaches made to understand MAE in a particular property often have their own implications on other properties and have therefore been critically examined in the literature. As examples, the requirement of the presence of isotope effects in electrodynamic theory, and the essentiality of the presence of non-bridging oxygen (NBO) sites in structural theories have been examined and shown to be incorrect[20–22]. Since MAE has a bearing on many technological applications of glasses (toughening of glass, control of dielectric properties, etc.)[1–4], it is necessary to examine this phenomenon in greater detail. Indeed the question

*For correspondence. (e-mail: kjrao@sscu.iisc.ernet.in)

whether the qualitative aspects of MAE are dependent on the nature of the glass itself, has not been clearly answered because MAE seems to be quite a general phenomenon occurring in both network and non-network glasses[1,3,23]. Of the several quantitative aspects, non-incidence of MAE below a critical total concentration of alkalies[3] and above some limiting temperatures[3], is also not well-understood. Inter-alkali distances vary as $c^{1/3}$, where c is the concentration of the alkali. The ratio of the average inter-alkali distances for two concentrations like 10 and 30% total alkali is only $(0.1/0.3)^{1/3} \sim 0.7$, and just this 30% increase in inter-alkali distance is enough to suppress MAE in alkali ion transport completely in borate glasses containing only 10% total alkali. Similarly, severe structural effects such as formation and collapse of $[GeO_{6/2}]^0$ units in germanate glasses[24] or formation and collapse of $[BO_{4/2}]^-$ units in borate glasses[25], do not seem to affect the incidence of MAE in these glasses. Therefore, further experimental and theoretical investigations appear essential in order to obtain new insights on the phenomenon of MAE.

Here, MAE in the properties of boro-tellurite glasses is examined. Both borate and tellurite glasses themselves exhibit interesting variations in structural features as a function of modification by alkalies. In B_2O_3 glass, addition of alkalies initially creates tetrahedrally coordinated boron, B_4^- ($\equiv [BO_{4/2}]^-$), till alkali concentration reaches nearly that of diborate. Above this concentration, B_4^- tetrahedra break down and both B_4^- and trigonal borons (B_3^0) together transform to charged two-bonded B_2^- ($\equiv[BO_{2/2}O]^-$) units[25,26]. Therefore, formation of NBO in the structure is delayed till the alkali concentration increases to nearly that of a diborate and eventually NBO concentration increases rapidly. Percentage of alkali required for this to happen, nevertheless, appears to vary with the nature of the alkali; the heavier alkalies bring about this change at higher concentrations[25]. In TeO_2, the structure consists of trigonal bipyramidal (tbp) units corresponding to $[TeO_{4/2}]^0$ ($\equiv T_4^0$). During modification by alkalies, T_4^0 units change to both T_4^- and (perhaps preferentially to) trigonal pyramidal (tp), $[TeOO_{1/2}O]^-$ ($\equiv T_3^-$) units. The latter leads to rapid collapse of three-dimensional connectivities in the glass. Boro-tellurite glasses, indeed, exhibit rich phenomena because of such complex speciation[27]. Such a glass host would be appropriate to examine MAE because a number of aspects surmised above can be examined even more definitively.

In this article, we have examined three different glass compositions (borate-rich glasses, tellurite-rich glasses and glasses with equal concentrations of borate and tellurite) containing 30% of total alkali ($Li_2O + Na_2O$). Several properties like densities and molar volumes, glass transition temperatures and heat capacities have been determined. Infrared, Raman and ^{11}B MAS NMR spectra have been examined to follow structural changes in mixed alkali glasses. D.c. and a.c. conductivities and dielectric relaxation behaviours have been analysed keeping in view the manifestation of MAE. In the following sections, the experimental procedures used are described and our observations (results) are presented and discussed. A new approach to conductivity and MAE is proposed on the premise that NBO–BO bond switching is the basic first step which induces alkali ion transport and MAE is a consequence of the variation of NBO–BO switching energetics.

Experimental section

Glasses were prepared by the conventional melt quenching method. The starting materials, Li_2CO_3 (Qualigens), Na_2CO_3 (Qualigens), H_3BO_3 (Qualigens) and TeO_2 (Aldrich; all of Analar grade) were mixed thoroughly by grinding in appropriate quantities so as to constitute a 10 g batch. The ground mixtures were heated in porcelain crucibles at 673 K for about 5 h in a muffle furnace to decompose Li_2CO_3, Na_2CO_3 and H_3BO_3. The batches were then melted at 1223 K for about 10 min, stirred to ensure homogeneity and quenched between stainless steel plates kept at room temperature. Using Li_2CO_3 and Na_2CO_3 is known to give glasses which exhibit properties identical to those obtained from oxides. Platinum crucible was not used in the preparation as it is found to be mildly reactive towards TeO_2 (ref. 28).

The amorphous nature of the glass samples was confirmed using X-ray diffraction (JEOL JOX-8P X-ray diffractometer). That the products were truly glasses was ascertained using Differential Scanning Calorimetry (DSC; Perkin-Elmer DSC-2). Thermal properties like glass transition temperature, T_g and heat capacity, C_P of the samples were also determined. Dry nitrogen was used as purge gas during DSC experiments. The C_P of the glasses was determined from room temperature up to temperatures well above T_g (limited only by the incidence of crystallization) using corresponding DSC data on single crystal sapphire (Al_2O_3; standard). The densities were determined using glass bits free of air bubbles and cracks (in $10\times$ magnification) through apparent weight-loss method. Xylene was used as the immersion fluid. Measured densities of well-annealed glasses were found to be accurate and reproducible to $\pm$ 0.001 g/cc. The molar volumes, $V_m = (W_m/\text{density})$, were calculated from density data, W_m being the corresponding formula weights.

The Fourier Transform Infrared (FTIR) spectra of the glasses were recorded between 4000 and 400 cm^{-1} on a Nicolet 740 FTIR spectrometer. KBr pellets containing the samples were used for the purpose. FT–Raman spectra were recorded on a Bruker IFS FT–Raman Spectrometer, using Nd : YAG (wavelength 1.064 μm) laser as exciting radiation. All spectra were recorded at 4 cm^{-1} resolution with an unpolarized beam. Spectra were recorded using an aluminium sample holder. Laser power was kept at 200 mW and typically 512 spectra were co-added to improve the signal-to-noise ratio. The spectra are in the temperature-reduced form[29], $I_{red} = I(\nu)/(1 + n(\nu))$, where $I(\nu)$ is the mea-

sured Raman intensity and $n(\nu)$ is the Bose distribution factor given by $n(\nu) = [\exp(hc\nu/k_BT) - 1]^{-1}$, ν is the Raman shift in cm^{-1}, c is the speed of light, T the absolute temperature, and h and k_B are the Planck and Boltzmann constants respectively. ^{11}B MAS NMR spectra were recorded on a Bruker MSL-300 solid-state high-resolution spectrometer operating at 90.4 MHz (magnetic field 7.05 T). 90° pulses of 5 μs were employed with a delay time of 10 s between pulses in all the experiments. A spinning speed of 7–10 kHz was employed. All the spectra were recorded at room temperature using freshly powdered samples.

Electrical conductivity measurements were carried out on a Hewlett–Packard HP4192A LF impedance-gain phase analyser (Hewlett–Packard, USA) from 10 Hz to 13 MHz in the temperature range of 298 to 600 K. A home-built cell assembly (having a two-terminal capacitor configuration and silver electrodes) was used for the measurements. The sample temperature was measured using a Pt–Rh thermocouple positioned close to the sample. The temperature was controlled using a Heatcon (Bangalore, India) temperature controller and the temperature constancy of ± 1 K was achieved in the entire range of measurements. Annealed circular glass bits coated with silver paint on both sides and having a thickness of about 0.1 cm and 1 cm diameter were used for measurements. The real (Z') and imaginary (Z'') parts of the complex impedance (Z^*) were obtained from the measured conductance and capacitance using the relations

$$Z' = G/(G^2 + \omega^2C^2),$$

$$Z'' = \omega C/(G^2 + \omega^2C^2),$$

where G is the conductance, C the parallel resistance and ω is the angular frequency. The real (ε') and imaginary (ε'') parts of the complex dielectric constant were calculated from the relations

Table 1. Designations, compositions, densities and molar volumes of mixed alkali boro-tellurite glasses, $30(Li,Na)_2O{\cdot}xB_2O_3{\cdot}(70–x)TeO_2$ ($20 \le x \le (50)$

Code	Composition				Density (g/cc)	Molar volume (cc)
	Li_2O	Na_2O	B_2O_3	TeO_2		
B1	30	00	50	20	2.941	25.74
B2	25	05	50	20	2.953	26.18
B3	15	15	50	20	2.968	27.12
B4	05	25	50	20	2.973	28.16
B5	00	30	50	20	2.948	28.94
T1	30	00	20	50	3.855	26.64
T2	25	05	20	50	3.859	27.02
T3	15	15	20	50	3.833	28.05
T4	05	25	20	50	3.786	29.24
T5	00	30	20	50	3.756	29.91
E1	30	00	35	35	3.394	26.28
E2	25	05	35	35	3.404	26.67
E3	15	15	35	35	3.418	27.50
E4	05	25	35	35	3.409	28.52
E5	00	30	35	35	3.404	29.03

$$\varepsilon' = Cd/\varepsilon_0A,$$

$$\varepsilon'' = \sigma/\omega\varepsilon_0,$$

where d is the sample thickness, A is the cross-sectional area, σ is the conductivity, and ε_0 is the permittivity of free space.

The data were also analysed using the electrical modulus formalism. The real (M') and imaginary (M'') parts of the complex electrical modulus ($M^* = 1/\varepsilon^*$) were obtained from ε' and ε'' values using the relation,

$$M' = \varepsilon'/((\varepsilon')^2 + (\varepsilon'')^2),$$

$$M'' = \varepsilon''/((\varepsilon')^2 + (\varepsilon'')^2).$$

Results

Glasses investigated in this work have been made with three combinations of the glass formers, B_2O_3 and TeO_2. The first B_2O_3-rich glasses (B series) correspond to B_2O_3 : TeO_2 ratio of 50 : 20 and the second TeO_2-rich glasses (T series) have a ratio of B_2O_3 : TeO_2 of 20 : 50. Glasses in which B_2O_3 : TeO_2 ratio is unity (= 35 : 35) are designated as the E series. In all the three series, total alkali content is 30% of the glass composition. Compositions are listed in Table 1.

Densities and molar volumes

Densities of the glasses at 25°C are shown in Figure 1 for the mixed alkali compositions for all the three series of glass. In all the three series, there is clear manifestation of MAE as density maxima. The difference between the minimum and the maximum glass densities is highest in tellurite-rich glasses, but the overall magnitude of MAE in density is small. The magnitudes of MAE reckoned as deviation from a linear variation in the three series of glasses are similar (~ 0.02 g/cc). The maxima occur at different values of inter-alkali proportions and shift towards sodium-rich side as in B_2O_3-rich compositions. It occurs at $[Li^+]/\{[Li^+] + [Na^+]\} = 0.5$ in the E series for which $[TeO_2]/\{[TeO_2] + [B_2O_3]\} = 0.5$.

Molar volumes (Figure 2) also exhibit MAE as nonlinear behaviour in mixed alkali compositions but with no maxima or minima. The range of molar volumes is 25.7 to about 29.7 cc (~ 4 cc) for all the three series of glasses. The change in volume is ~ 3.2 cc in the B series and only ~ 2.8 cc in the E series.

Thermal properties

The glass transition temperatures (T_g) for the three series are given in Table 2. T_gs are highest for B_2O_3-rich series and inter-alkali variation plots (Figure 3 *a–c*) reveal manifestation of MAE in all the three series. The heat capacity measurements were used to determine T_g, widths

of the glass transition temperature ΔT_g and also the heat capacity jumps ΔC_P. These quantities are listed in Table 2. There is no clear manifestation of mixed alkali behaviour in ΔC_P. However, thermodynamic $F_{1/2}$ fragilities[30,31] calculated using the formula, $F_{1/2} = [0.151 - x]/[0.151 + x]$, where $x = \Delta T_g/T_g$, revealed manifestation of MAE and the behaviour is shown in Figure 3 *d*.

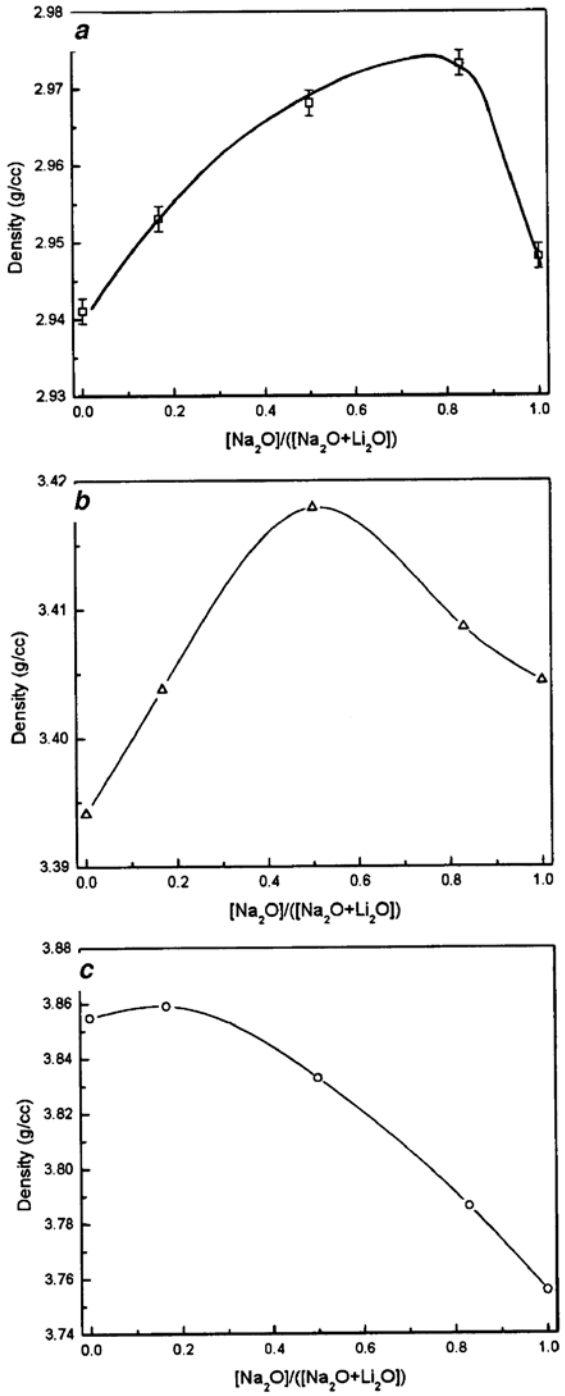

Figure 1. Variation of density as a function of mixed alkali composition for *a*, B series, *b*, E series and *c*, T series of glasses.

Spectroscopic studies

The IR spectra of the three series of glasses are shown together in Figure 4. The two major peaks in the region 1000–1400 cm^{-1} in the B series arise from tetrahedral (~ 1000 cm^{-1}) and trigonal boron (~ 1400 cm^{-1}). The third major absorption band in the 600–900 cm^{-1} region is constituted of both borate-bending and tellurite-stretching vibrations. All the IR bands exhibit shifts and splittings as a function of inter-alkali variation. However, it is difficult to deconvolute the spectra and clearly delineate the changes. The peak in the 1400 cm^{-1} region is associated only with the stretching vibration of B_3 units. The peak position of this band shifts in the manner shown in Figure 4 *d*. In all the three series, the frequency shift exhibits a maximum in the inter-alkali region thereby indicating the manifestation of MAE in vibrational spectra. Alkali ratio also appears to influence the position of the shift maximum. In the *T* series, downward shift on the Na-rich side is the highest, which suggests a weakening of the stretching vibrations of B_3 units.

The reduced Raman spectra of the three glass series are shown together in Figure 5. Raman spectra are particularly well-suited for studying tellurite species because peaks in the region of 600 to 900 cm^{-1} are generally attributed only to tellurite and not to the borate species which, by comparison, scatter weakly. The integrated intensities of these peaks obtained under identical conditions for the T5 and B5 glasses are in the ratio 1.8/1.0 compared to the value of 1.5/1.0 expected when tellurite scattering is dominant, suggesting that these peaks are largely due to tellurite species. In the borate-rich species, the peak occurs at 786 cm^{-1} with only a weak shoulder-like feature at 710 cm^{-1} (more clearly evident in B5), whereas in the *T* series the main peak is slightly red-shifted to 778 cm^{-1} and a distinct peak centred around 679 cm^{-1} appears as a split-off (from

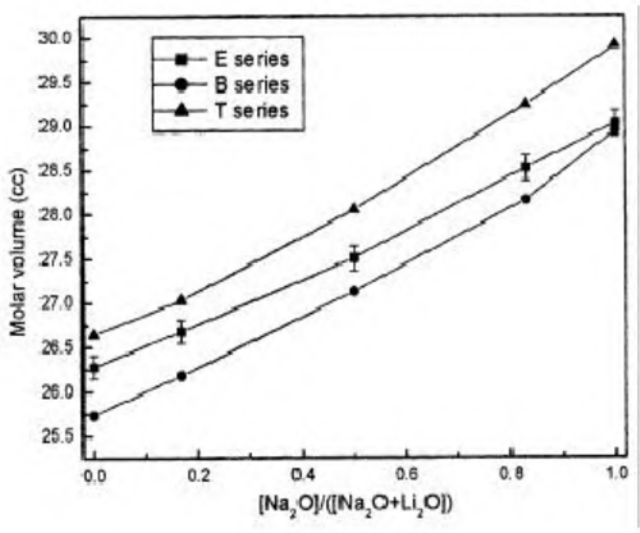

Figure 2. Variation of molar volume as a function of mixed alkali composition for mixed alkali boro-tellurite glasses.

the 778 cm^{-1} peak) feature (see T5). These peaks are generally attributed to tbp (778 cm^{-1}) and tp (679 cm^{-1}) structural species in tellurites[32–35]. It is important to note that the concentration of tp species increases towards Na-rich compositions in the glasses. Both IR and Raman spectroscopic features exhibited by the glasses in the E series are intermediate between those in the B and T series, suggesting a continuous variation of spectroscopic features and hence of the structural make up of the glass.

HR MAS NMR spectra of ^{11}B obtained for the three series are shown together in Figure 6. The spectra indicate the presence of both B_3 and B_4 species (the un-superscripted B_3 represents ($B_3^0 + B_2^-$) and $B_4 \equiv B_4^-$). The peak areas were analysed and concentration ratios, $N_4 = [B_4]/\{[B_3] + [B_4]\}$ were calculated by procedures described elsewhere[36]. The spectra in Figure 6 *a–c* reveal that the side-band intensities are quite low (borate species are in highly symmetrical positions) and therefore, the evaluation of N_4 is assumed to be reasonably accurate. Variation of N_4 as a function of inter-alkali variation for the three series is shown together in Figure 6 *d*. It can also be seen from Figure 6 *d* that although N_4 is sensitive to the ratio of B_2O_3 to TeO_2 in the glass, it is not much affected by inter-alkali variation. Also, lower ratio of B_2O_3 to TeO_2 in the glass favours retention of B_4 in the glasses to a high degree.

Conductivity and dielectric relaxation

The d.c. conductivities obtained from impedance plots for the three series of glasses at four different temperatures are shown together in Figure 7. The variations clearly reveal the manifestation of MAE in d.c. conductivity. At 463 K, the strength of MAE in conductivity is about 2 orders of magnitude and the conductivity minima occur generally in Na-rich compositions. The strength of the MAE decreases at higher temperatures. The dotted lines in Figure 7 *c* correspond to measurements made at and just above T_g, indicating persistence of MAE even at high temperatures although its magnitude is much lower. The

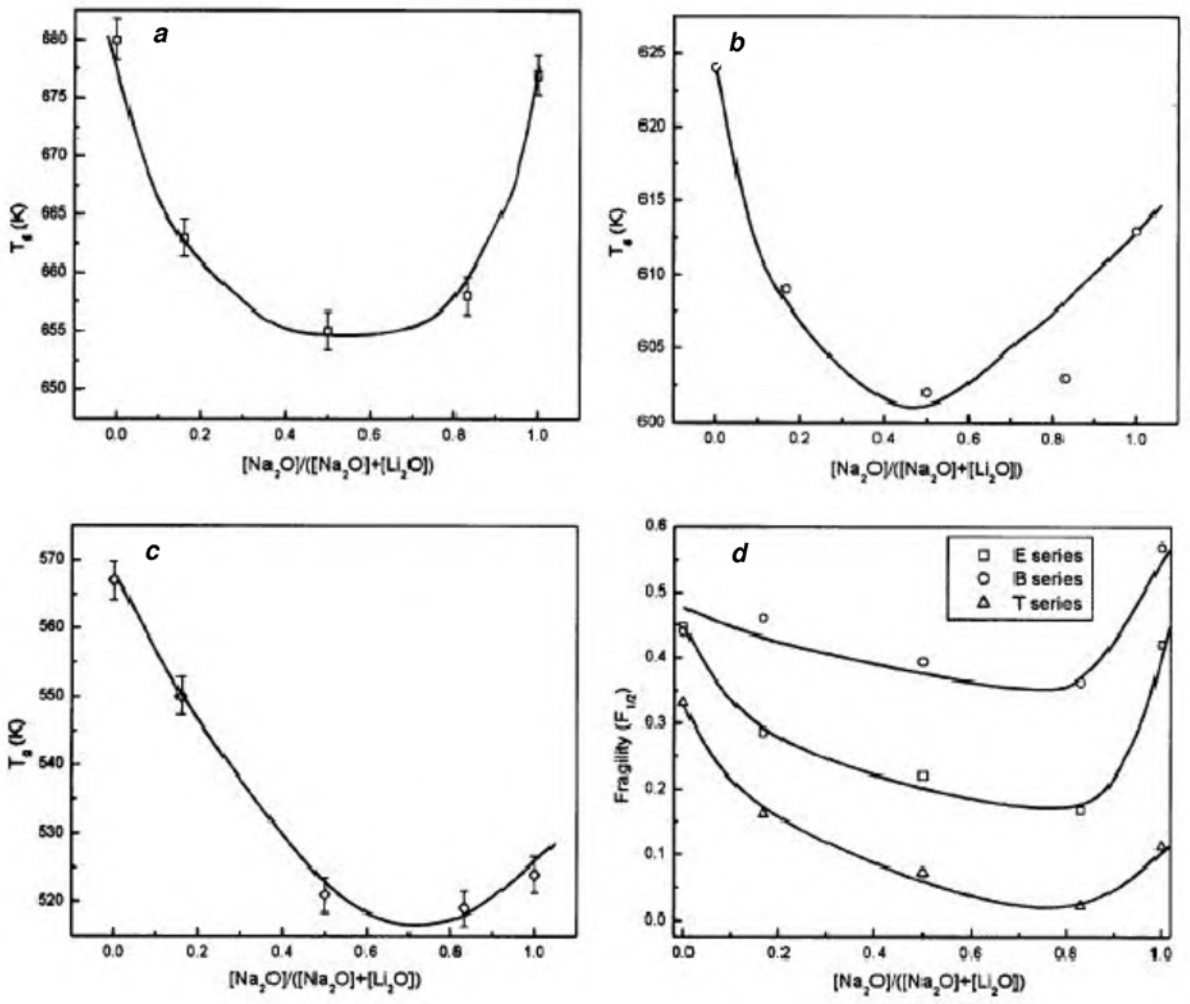

Figure 3. Variation of T_g as a function of mixed alkali composition for ***a***, B series, ***b***, E series, and ***c***, T series of glasses. ***d***, Variation of $F_{1/2}$ fragilities for mixed alkali boro-tellurite glasses.

variation of conductivity activation barriers (evaluated using Arrhenius plots) with mixed alkali composition is shown in Figure 7 *d*, which again reveals MAE. The magnitude of MAE in the activation barrier is the highest in tellurite-rich glasses.

AC conductivities of all the glasses were studied at various temperatures up to T_g. Typical ln σ vs ln ω plots are shown in Figure 8 *a*. Such plots were fitted to a two-term power-law expression[37–40], $\sigma = \sigma_0 + A\omega^s$. The variation of s itself as a function of temperature is examined in Figure 8 *b* for all the glasses. The values of s generally lie in a narrow range of 0.5 to 0.7 (Jonscher regime)[37], although the dispersion of s values is somewhat higher at still higher temperatures. On a closer examination it is found that in several glasses, particularly in TeO_2-rich glasses, s values exhibit shallow minima and are shown separately in Figure 8 *c* on an expanded scale. Figure 8 *d* shows the locus of the temperatures (T_{min}) of s_{min} in typical mixed alkali plot, which again reveals MAE.

Behaviour of the covariant dielectric features has also been examined. For this purpose, dielectric moduli have been calculated using standard expressions[41] and typical M'' vs log(ω) plots are shown in Figure 9 *a*. The values of β were calculated assuming that M'' variation in frequency domain is due to stretched exponential nature of relaxation, $\phi = \phi_0 \exp\{-(t/\tau)^{\beta}\}$, in the time domain, and using the empirical relation between β and full-width-at-half-maximum (FWHM) values of M'' peaks[42]. Variation of β for all the glasses in the three different series at various temperatures is shown together in Figure 9 *b*. β values are generally confined to the range of 0.5 to 0.7. β values therefore appear to be generally unaffected by temperature. Variation of β is shown in a mixed alkali plot in Figure 9 *c*, which indicates that β is unaffected by inter-alkali variations in all the three series of glasses. We have also examined time–temperature superposition of the imaginary part of the modulii for all the glasses and a typical plot is shown in Figure 9 *d* for the case of B3 glass. The excellent superposition confirms that the transport mechanism in all the glasses remains the same and is unaffected by temperature.

Table 2. Thermal properties and fragilities of mixed alkali borotellurite glasses, $30(Li,Na)_2O{\cdot}xB_2O_3{\cdot}(70–x)TeO_2 (20 \le x \le 50)$

Code	ΔC_P	ΔT_g	T_g(K)	C_P (J/K/mol)		$F_{1/2}$
				C_P	C_P(3nR)	
B1	63.3	40	680	93.4		0.44
B2	71.3	37	663	90.4		0.46
B3	67.3	43	655	95.5	99.77	0.39
B4	60.0	46	657	92.5		0.37
B5	50.0	28	677	94.3		0.57
T1	47.2	43	567	76.0		0.33
T2	47.9	60	550	73.9		0.16
T3	35.9	62	521	66.2	84.80	0.12
T4	43.5	68	519	65.1		0.07
T5	51.6	63	524	63.1		0.11
E1	84.6	36	624	86.4		0.45
E2	76.3	51	609	90.5		0.29
E3	64.4	58	602	92.9	92.28	0.22
E4	47.1	66	603	89.9		0.16
E5	45.4	37	613	93.1		0.43

In summary, MAE is seen to manifest in several properties in the boro-tellurite glasses; in densities as a maximum, in molar volumes as a nonlinear increase, in glass transition temperatures as a maximum, in fragilities as a minimum, in vibrational frequencies (IR) as a maximum, in d.c. conductivities as a minimum, in d.c. conductivity activation barriers as a maximum and as maximum of T_{min} corresponding to s_{min}. But both frequency exponent s and stretching exponent β, over a wide range of compositions and temperatures (in all the three series), are unaffected by inter-alkali variations.

Discussion

Densities and molar volumes

MAE in densities can be related to structural features. As noted earlier, modification by alkali oxides initially results in the formation of tetrahedral B_4^- units. With increasing alkali, N_4 increases to a maximum of ~ 0.5, where the alkali to B_2O_3 ratio is ~ 1 : 2. When alkali concentration increases further, a rapid decrease of N_4 is observed due to conversion of B_4^- to B_3^-. The maximum value of N_4 is affected by the size of the alkali ion, and in the boro-tellurite system it is also affected by the presence of tp units. This is because tp units stabilize B_4 units by causing their physical separation in the glass structure[27]. TeO_2 itself is known to produce B_4 units in alkali-free binary $B_2O_3{\cdot}TeO_2$ glasses[34], which is possible only if tp units provide the required additional coordination to boron, presumably by the conversion of a terminal oxygen to a bridging oxygen (BO); $[TeOO_{2/2}]^0$ is converted to $[TeO_{3/2}]^+(T_3^+)$ in the structure. Therefore, in the presence of TeO_2 in the glass, N_4 values can be expected to be higher. The structure of the glasses investigated here consists of several species. These species may be represented by the usual notation, B_m^n and T_m^n, where B and T stand for boron and tellurium, and n and m are the charge and connectivity in the structure. The average dimensionality of the glass structure is determined by the composition in terms of structural units because the constituent structural units have different connectivities. T_4^0, T_3^- and B_4^- increase the dimensionality of the network, while T_2^0, T_1^-, B_3^0 and B_2^- decrease it. Since the total alkali is constant, the magnitude of modification is constant in all the glasses. But the extent of modification on the two glass formers, B_2O_3 and TeO_2 can be different and that determines the dimensionality of the glass structure. While modification on TeO_2 (whether $T_4^0 \rightarrow T_3^- \rightarrow T_1^-$ or $T_2^0 \rightarrow T_1^-$) decreases the dimensionality irrespective of alkali concentration, modification of B_2O_3 may cause both increase ($B_3^0 \rightarrow B_4^-$) and

decrease ($B_3^0 \rightarrow B_2^-$) of dimensionality. $B_4^- \rightarrow B_2^-$ and $T_4^0 \rightarrow T_1^-$ conversions cause a drastic change in dimensionality. Further, the coordination requirements of alkali ions (Li^+ or Na^+) are different because of the different sizes. Together, the nature of speciation and the coordination requirements of alkali ions determine the packing efficiency and hence the densities.

From Figure 1, it is seen that the density maximum occurs in the E series ($[B_2O_3]/[TeO_2] = 1$) at 50% Na_2O. It shifts to lower Na_2O (around 20%) in the T series of glasses and higher Na_2O (around 75%) in the B series of glasses. Borate-rich glasses have the lowest B_4^- concentration (Figure 6 *d*) and the highest ($T_4^0 + T_3^-$) (tbp) concentration (Figure 5 *c*). Thus, a low ratio of B_4^- to ($T_4^0 + T_3^-$) appears to be associated with a high ratio of Na^+ to Li^+. In complete contrast to this, in the tellurite-rich T series of glasses, B_4^- is maximum although ($T_2^0 + T_1^-$) also increases to higher values (T_4^0 and T_3^- decrease correspondingly). Thus a higher ratio of B_4^- to ($T_4^0 + T_3^-$) is associated with lower ratio of Na^+ to Li^+ in the T series of glasses. We recall that T_4^0 (T_3^-) $\rightarrow T_2^0$ (T_1^-) (tbp to tp) leads to drastic reduction in dimensionality ($T_1^- \equiv [TeOO_{1/2}O]^-$ units, are chain terminators) and affects the nature of packing. Therefore, the effect on the molar volume behaviour can be anticipated as follows. TeO_2-rich glasses should possess a more open structure because of large N_4 concentration and therefore larger molar volume. On the other hand, borate-rich glasses may be expected to possess the lowest molar volumes because N_4 concentration is much lower. The E series of glasses are expected to exhi-

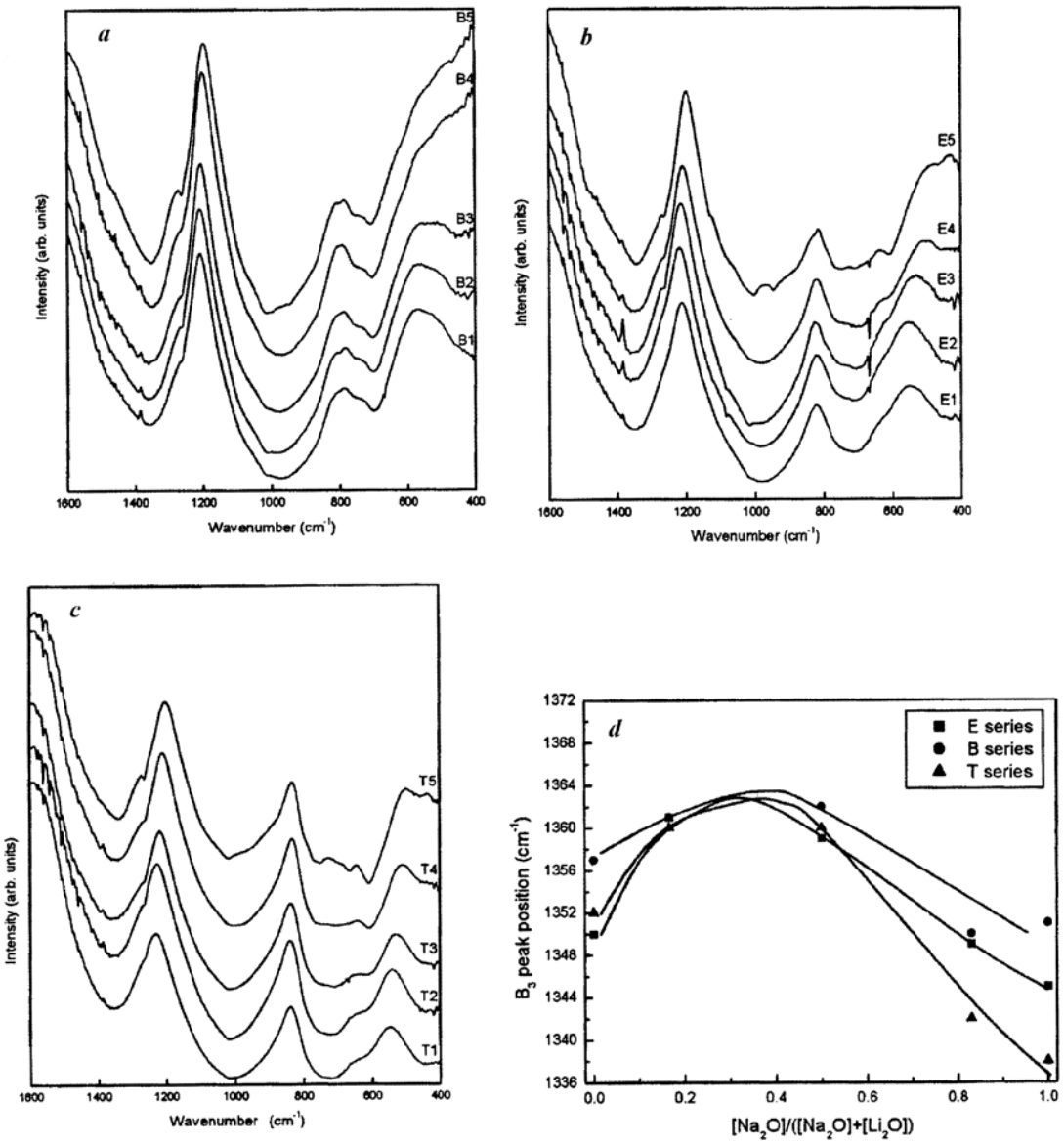

Figure 4. IR spectra of *a*, B series, *b*, E series and *c*, T series of glasses. *d*, Variation of B_3 peak position as a function of mixed alkali composition for mixed alkali boro-tellurite glasses.

bit intermediate behaviour. This is clearly seen in Figure 2. Further, Na^+-rich compositions are expected to consist of greater proportion of B_4^- or T_4^0 (and T_3^-), which leads to even more open structures. Therefore, the corresponding molar volumes are expected to increase more rapidly towards the Na^+-rich side, which is also consistent with experiments (Figure 2). The variation of molar volumes is slightly nonlinear and can be fitted to a quadratic equation of the type $a_1 + a_2x + a_3x^2$, where $x = [Na_2O]/\{[Na_2O] + [Li_2O]\}$. The mole fraction weighted 'molecular weights' of the glasses, however, vary linearly and can be fitted to an expression like $b_1 + b_2x$. The density, ρ, is therefore a function of the form, $\rho = (b_1 + b_2x)/(a_1 + a_2x + a_3x^2)$. The differential of this, $(d\rho/dx)$, when equated to zero, gives a real value of x such that $0 < x < 1.0$. Therefore, the occurrence of density maximum is accounted for. Although this explains MAE, the quantitative agreement between calculated and observed values of x is poor. Further, the quadratic variation of molar volume can be explained qualitatively. Volume increase is determined by the formation of B_4^- and T_3^- or T_4^0 units. Concentration of both B_4^- and T_3^- or T_4^0 is proportional to Na_2O concentration. Thus it is not surprising that the volume increase is quadratic, since both B_4^- ($\propto x$) and T_3^-/T_4^0 ($\propto x$) increase simultaneously.

T_g and fragilities

Borate-rich glasses exhibit the highest values of T_g and tellurite-rich glasses the lowest. In the E series, T_gs lie in the intermediate range. The general decrease in T_g values with the substitution of B_2O_3 on a molar basis by TeO_2 is understandable in terms of weakening of the lattice, because a larger number of stronger B–O bonds are replaced by the fewer and relatively weaker Te–O bonds. MAE in T_g by inter-alkali substitution may have at least two important origins. Increased configurational entropy due to the presence of two alkalies may lower the liquidus temperature in mixed alkali compositions and hence give rise to T_g minimum in inter-alkali region. Secondly, the different preferences of coordination of the alkalies enhance the possible alkali–NBO complexions in the molten state, which also suppresses the liquidus temperatures, and thus causes a minimum in T_g. NBO dynamics plays a vital role in this context, which we will discuss later.

The fragility behaviour in Figure 3 *d* reveals MAE. The fragility minima, however, do not occur at the same compositions where density maxima are observed in mixed-alkali plots. The fragility minima also seem to occur in Na_2O-rich regions in all the three systems. Also, tellurite-rich glasses are the least fragile. TeO_2 itself is expected[31] to exhibit a low fragility value of ~ 0.06. The fragility expression suggests that a combination of T_g minima and/or ΔT_g maxima can give rise to such fragility minima. As noted earlier, vibrational spectroscopy indicates that as Na_2O is increased there should be a monotonic increase in tp units. This brings about a sharp and continuous decrease of connectivity in the glass structure. Intuitively, we see that this causes local heterogeneities in the structure and hence a diffuseness of T_g. Therefore, ΔT_g increases. The combination of T_g minimum effect and diffuseness of T_g accounts for the shallow minima in $F_{1/2}$, which expectedly occurs in Na^+-rich regions.

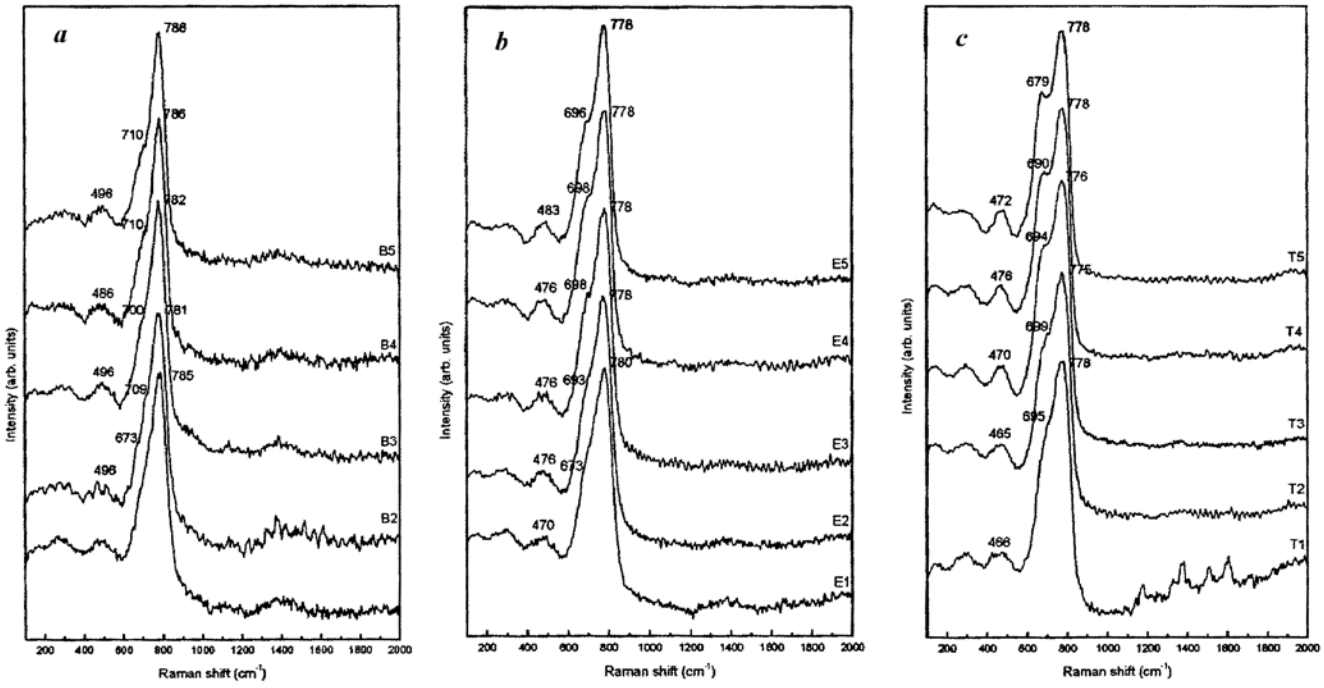

Figure 5. Reduced Raman spectra of ***a***, B series, ***b***, E series and ***c***, T series of glasses.

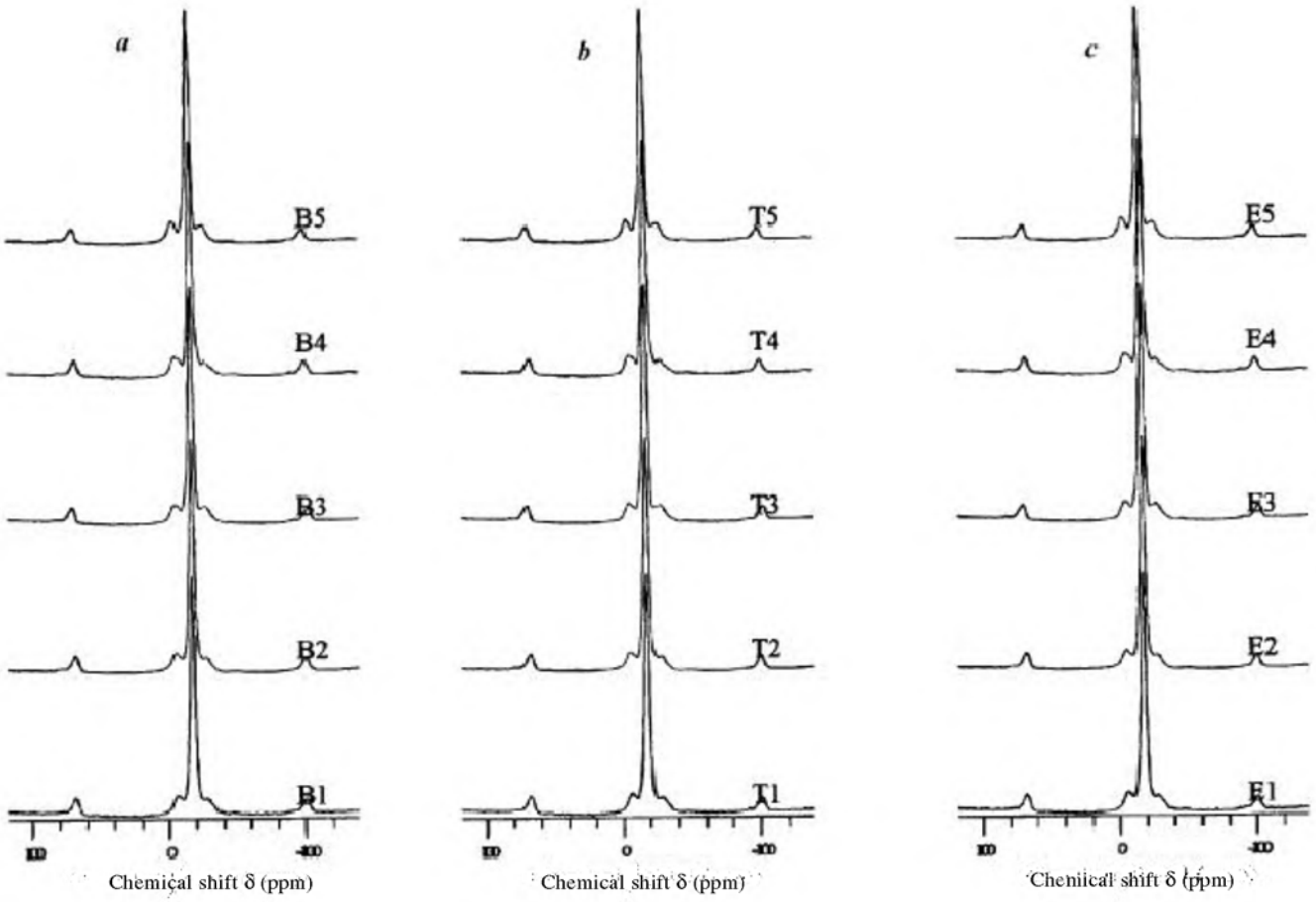

Figure 6. ^{11}B HR MAS NMR spectra of ***a***, B series, ***b***, T series and ***c***, E series of glasses.

Spectroscopic studies

As pointed out in the previous section, absorption peak in the region of 1200 cm^{-1} arises from trigonal borons, B_3^0 and B_2^-. The variation of the position of this peak (Figure 4 *d*) reveals that this frequency increases in mixed alkali compositions, suggesting a greater stabilization of B_3 units. It is natural to associate this stabilization with more efficient packing around B_3 units in mixed alkali compositions arising from an optimal mixing of Li^+ and Na^+ ions. The stretching frequency of B_3 units undergoes a red-shift when the planarity of the B_3 unit is affected by the build-up of electron density in its vacant 2p orbital. Alkali ions (and rather effectively, Li^+ ions) prevent such build-up in both B_3^0 or B_2^- units when they are present in their immediate vicinity (we will see later that there may be only B_2^- units in the B series of glasses, unlike in the E and T series). This is consistent with Figure 4 *d*, where this stretching frequency is seen to be higher when only Li_2O is present than when only Na_2O is present. The additional stabilization indicated by maximum in B_3 frequencies in the mixed alkali compositions may arise from optimal geometrical packing, which causes further relaxation of the environment of B_3 units. Also, in borate-rich glasses containing B_3 and B_4^- units, presence of dissimilar alkali ions may help such optimal packing and geometric stabilization. The B_3 stretching frequencies are

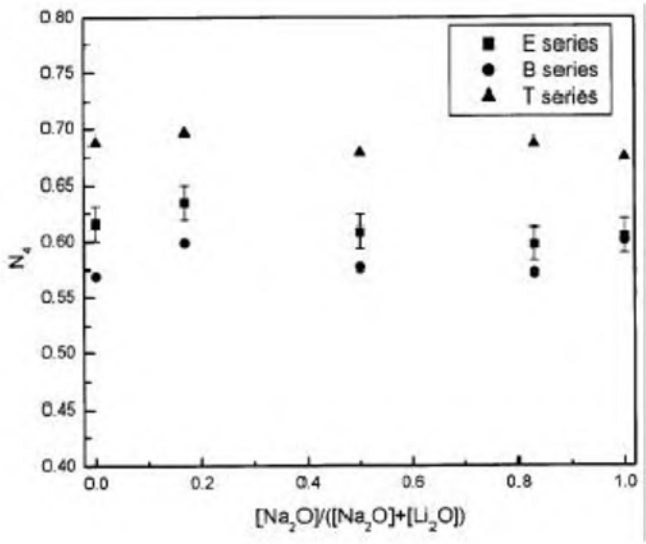

Figure 6. ***d***, Variation of N_4 as a function of mixed alkali composition for mixed alkali boro-tellurite glasses. Error bar has the same magnitude for all the three series.

therefore high. However, in Na-rich glasses, formation of terminal tp units ($[TeOO_{1/2}O]^-$) enhances the chances for additional oxygen coordination to B_3 units. This causes significant lowering of B_3 frequency, as evident from Figure 4 *a*. The decrease in planarity of B_3 units in the latter situation is weakly evident in the gradual splitting of B_3 peaks in T4 and T5 because of reduced symmetry of B_3 units from D_{3h} to C_{2v}.

The only feature of interest to MAE noticed in reduced Raman spectra of the glasses is the formation of tp units in Na-rich glasses, which is clearly revealed by the emergence of 679 cm^{-1} feature from the shoulder region of 730 cm^{-1} peak. In TeO_2-rich glasses, increased concentration of T_1^- units increases the chances for distortion of B_3 units, which therefore corroborates the reason given above for the observed red-shift of B_3(also B_2^-) stretching frequencies.

^{11}B MAS NMR results have revealed an interesting phenomenon that has direct bearing on MAE. First of all, N_4 values are significantly higher than those observed in any binary borate glasses. The unit composition of the B series of glasses being $30(Li,Na)_2O{\cdot}50\ B_2O_3{\cdot}20TeO_2$, to start with, there are 100 BO_3 units of which 60 may be considered as converted to $[BO_{4/2}]^-$, if all of 30 O_2^- from $(Li,Na)_2O$ are used up by B_2O_3 for its modification. The expected maximum value of N_4 is equal to 60/(60 + 40) = 0.6, which is nearly what is observed (Figure 6 *d*). This value of N_4 (= 0.6) is higher than the normal N_4 value (= 0.5) and can be attributed to stabilization of B_4^- in the presence of TeO_2, as discussed elsewhere[27,31]. In TeO_2-rich glasses, the concentration of B_4^- units is even higher. This seems to be a consequence of (i) the availability of higher-than-required modifier concentration (30 Li_2O for 20 B_2O_3) and (ii) the presence of significant concentration of T_1^- units, which stabilize B_4^- units by isolating them from other borate units. N_4 reaches high values of ~ 0.7 in the T series of glasses. It may be noted that in any given series of glasses, N_4 values themselves remain

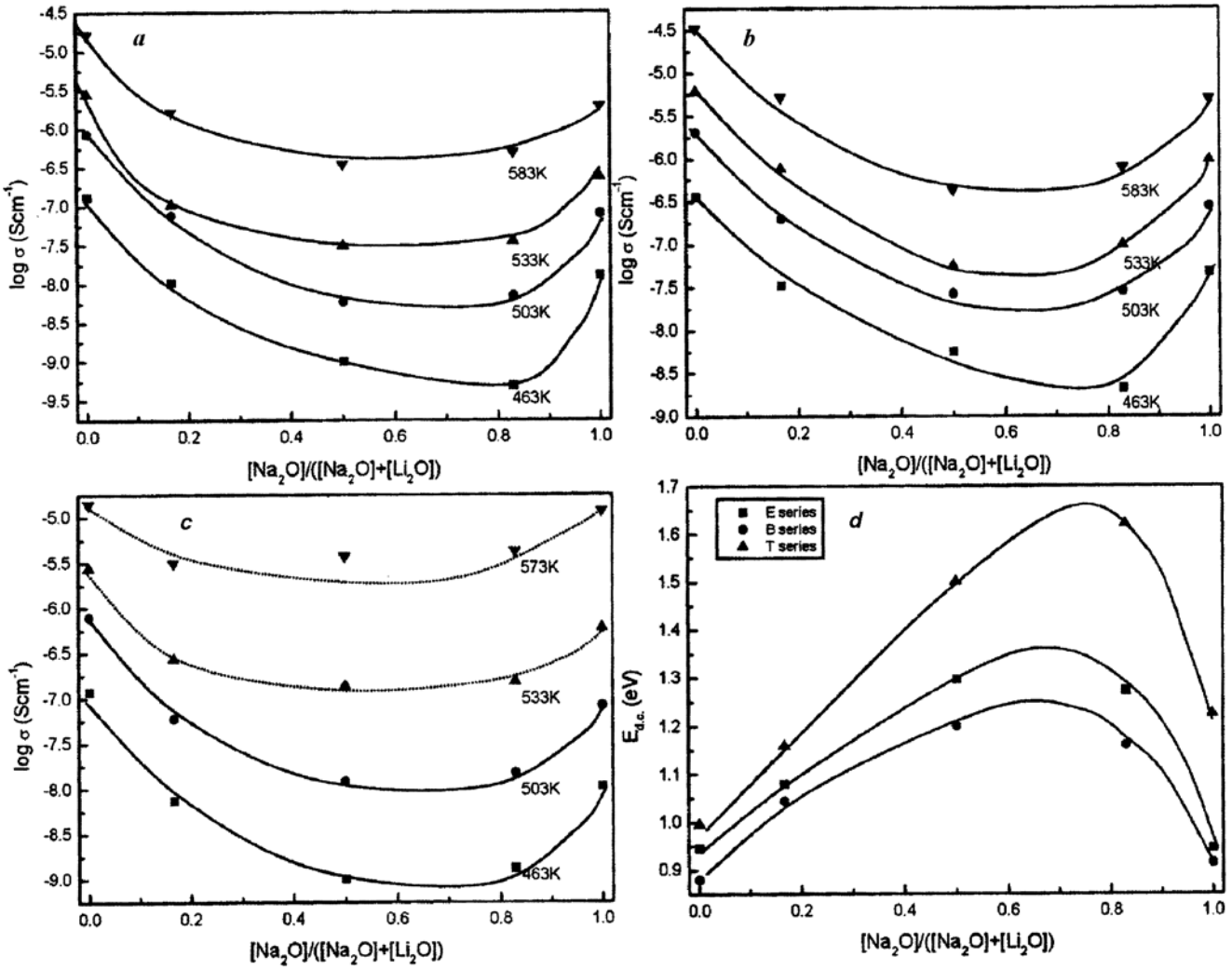

Figure 7. Variation of log ($\sigma_{d.c.}$) as a function of mixed alkali composition for *a*, B series, *b*, E series and *c*, T series of glasses. *d*, Variation of the activation barrier, $E_{d.c.}$ as a function of mixed alkali composition for mixed alkali boro-tellurite glasses. Dotted lines in *c* indicate the temperatures are above T_g.

essentially unaffected by inter-alkali variations. But the structural effects which they bring about cause MAE in densities, IR spectral features, etc. The N_4 values in the E series are between those of the B and the T series. However, in the B series, it is curious that all of the modifier oxygen is used up in the $B_3 \rightarrow B_4$ conversion in spite of TeO_2 having slightly higher molecular electronegativity ($\chi = 2.92$) than B_2O_3 ($\chi = 2.88$). This is perhaps a limitation of the electronegativity approach[43].

Conductivity studies

The most important manifestation of MAE is in d.c. conductivities (Figure 7 *a–c*). Approximately two orders of magnitude dip has been observed in $\sigma_{d.c.}$ values. Correspondingly, maxima are observed in activation energies (Figure 7 *d*) in mixed alkali regions. AC conductivities and $M''(\omega)$ of the mixed alkali glasses measured as a function of both temperature and frequency, however, do not reveal any features such as nonlinear variations in either *s* or β attributable to MAE. Figure 8 *a* (glass B_3) is an illustration of the essentially universal behaviour of $\sigma(\omega)$ of the glasses. The values of *s* examined both as a function of temperature and composition as noted earlier, are generally those expected from Jonscher-type dielectrics[37]. The temperature behaviour of *s*, particularly in the T series, however, exhibits shallow s_{min} (Figure 8 *c*) and, as noted earlier, the locus of these minima exhibits a mixed alkali maximum (Figure 8 *c*). The appearance of s_{min} has been widely discussed in the literature[4,44–47]. It is a consequence of the difference in the activation barriers obtained from relaxation frequencies (diffusion-independent barrier, *W*) and d.c. conductivities (diffusion-dependent barrier, $E_{d.c.}$). Generally, $W\text{-}E_{d.c.}$ is positive and a minimum occurs at a temperature T_{min}, where $W\text{-}E_{d.c.} = kT_{min}$ as may be inferred from diffusion relaxation[47–49]

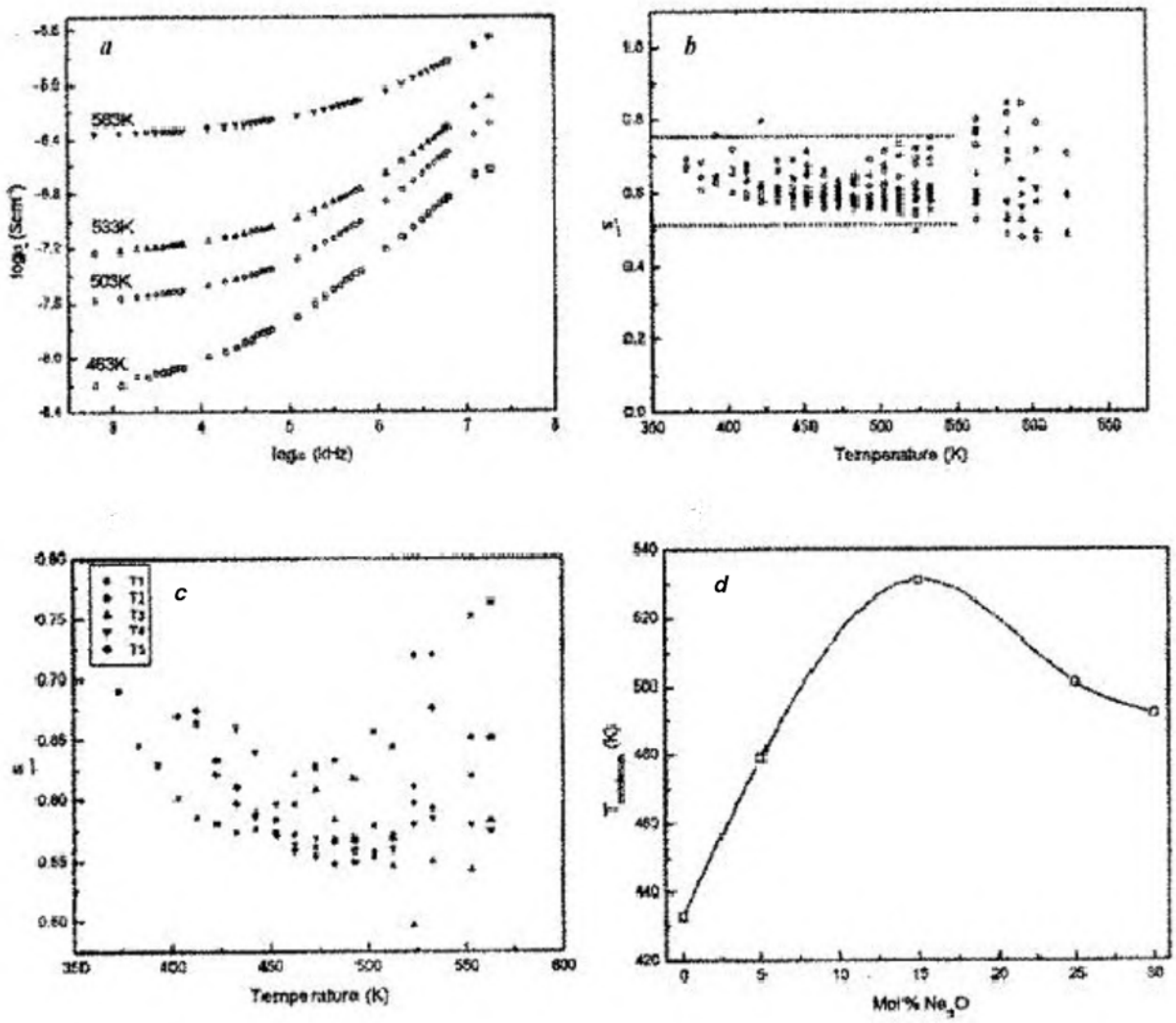

Figure 8. ***a***, Typical a.c. conductivity plots composition B3, at different temperatures. Variation of the power law exponent *s* as a function of temperature for ***b***, all the glasses and ***c***, T series of glasses. ***d***, Variation of T_{min} as a function of mixed alkali composition for T series of glasses.

and vacancy models[50–52]. Further, the magnitude of s_{min} itself is generally related to the d.c. conductivity[52,53], being lower when the conductivity is higher. Thus we would expect s_{min} or correspondingly T_{min} (temperature corresponding to s_{min}) to exhibit an anti-correlation to the d.c. conductivities in mixed alkali region, as indeed evident from Figure 8 *d*. But the overall spread of s values itself is notably low. This is indicative of the fact that the temperature dependence of the relaxation time, τ, and the diffusion coefficient, D, are roughly similar in magnitude but opposite in sign as required by the relation, $s = (D\tau/l_0^2)^{1/2}$ (l_0 is the hopping distance, which for constant alkali concentrations can be treated as invariant)[53]. Since $\sigma_{d.c.}$ is related to D through the Nernst–Einstein relation, $\sigma_{d.c.} = ne^2D/kT$, $\sigma_{d.c.}$ and τ are similarly anti-correlated.

The behaviour of M'' of the glasses as a function of composition and temperature supplements the behaviour of s. Figure 9 *a* shows M'' variation as a function of log ω for a typical case of borate-rich mixed alkali glass. The corresponding reduced plot of M''/M''(max) versus $\ln(f/f_0)$ (Figure 9 *d*) reveals excellent superposition even at very high frequencies. Similar behaviour is found in other series of glasses also. Therefore, the conduction mechanism remains the same throughout the measurement temperatures for all the compositions. A rather revealing fact is contained in Figure 9 *c*. The variation of β at 503 K, plotted as a function of mixed alkali parameter, is clearly insensitive to alkali interchange. In fact, β values for all the glasses as a function of temperature shown together in Figure 9 *b*, are also nearly constant with an average value of 0.6. As a consequence, there is a good collapse of M''/M''(max) versus $\log(f/f_0)$ plots (Figure 10) shown for 225 sets of datapoints obtained from measurements on 15 glass compositions over 15 different temperatures.

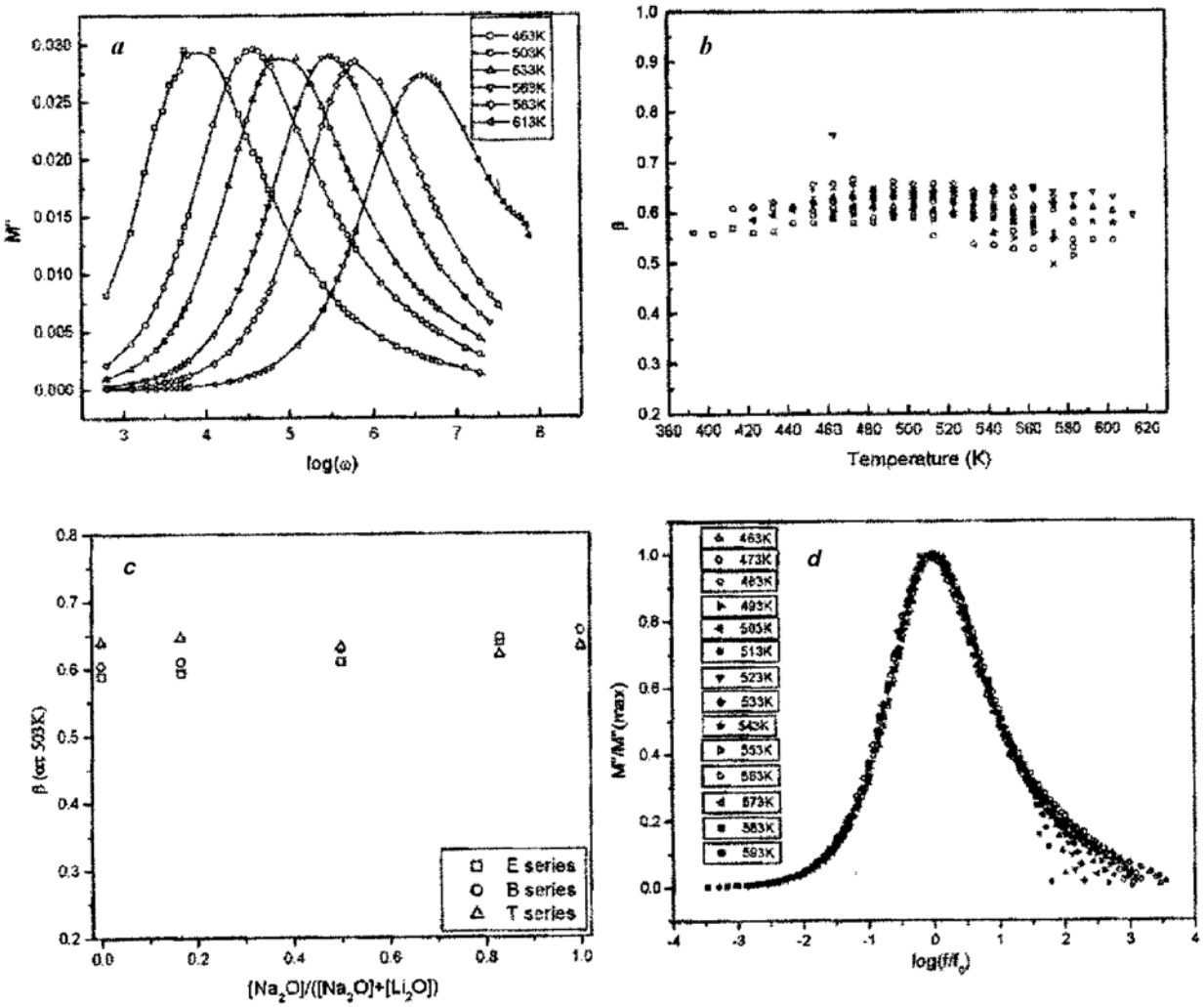

Figure 9. *a*, Typical plot of variation of imaginary M'', part of the electrical modulus with frequency for B_3 glass. *b*, Variation of the stretched exponent β with temperature for all the glasses. *c*, Variation of β at 503 K, as a function of mixed alkali composition. *d*, Typical normalized plot of M'' against normalized frequency for the glass B3.

The spread in β values is even lower than in *s* values. The near insensitivity of β and *s* towards inter-alkali variations is curious. There seem to be no other literature reports which have discussed this behaviour. Chen *et al.*[54], who made measurements in mixed alkali phosphate glasses, made a similar observation regarding the constancy of β. Theories like those of Ngai and co-workers[55,56] anticipate β to be sensitive to inter-cation interactions which must be present according to most theories of MAE. Therefore, both *s* and β are insensitive to inter-alkali variation and the origin of this behaviour needs to be understood. The basic features of the theory of ion transport in alkali-modified oxide glasses are briefly re-examined in order to find the necessary alterations to the theory, which may rationalize our observations of MAE.

DC conductivities exhibit minima in mixed alkali glasses and it is generally assumed that the minimum marks the composition on either side of which the transport is dominated by the majority alkali ions. Conductivity analysis also reveals a corresponding maximum in activation barrier. It is implied in this observation that the measured activation energy is common to both the alkali ions. This is a common barrier for conduction, because Arrhenius plots of $\sigma_{d.c.}$ versus $1000/T$ are quite linear. In the neighbourhood of the minimum conductivity, both alkali ions contribute similarly to measured $\sigma_{d.c.}$. But $\sigma_{d.c.}$ is not expressible as a sum of the two conductvities, $\sigma_{d.c.}(1) + \sigma_{d.c.}(2)$, where 1 and 2 represent the two alkali ions, because it would be inconsistent with the observed single activation barrier in the entire composition range.

$$\sigma_{d.c.} = \sigma_0(1)\exp\left(-\frac{E_a(1)}{RT}\right) + \sigma_0(2)\exp\left(-\frac{E_a(2)}{RT}\right) \neq \sigma_0 \exp\left(-\frac{E_a}{RT}\right).$$

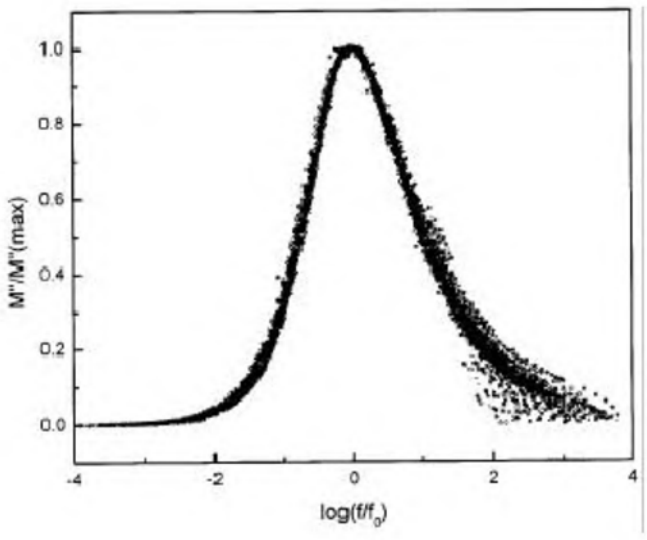

Figure 10. Master plot exhibiting the collapse of M'' against normalized frequency for all the glasses.

But, it appears fairly convincing from Monte Carlo and molecular dynamics (MD) simulations that the alkali ions migrate independently of each other and prefer chosen and independent migration paths because they exhibit site selectivity[7,8,57–59]. In MD simulations, this has been clearly brought out using powerful van Hove correlation functions.

Similarly, in a.c. conductivities, the two alkali ions should have given rise to some signature of their independent contribution towards total transport either in power law conductivity analysis as two different *s* values or in the modulii analysis as two different β values (with corresponding distortions of the shapes of the M'' plots), and neither has been observed. Inter-alkali interaction is also not observed because β is found to be quite insensitive. Therefore, an understanding of MAE in conductivity studies requires more than the structural and bonding considerations which we found adequate to understand MAE in other properties like density, vibrational spectra, etc. as discussed above.

In ion transport theories, it is generally assumed that the cations move into equivalent sites, which are in essence, equivalent NBO environments[12,60]. This is because the largest contribution to energetics of the alkali ion in its site is from coulombic interaction with the NBOs. The average distance between such environments or sites is a function of modification or alkali concentration (c), and varies as $c^{1/3}$. Since the NBOs and alkali ions are numerically equal and are always present together in the lowest energy configuration, the presence of an empty equivalent site invoked in transport theories is only a convenient assumption. We feel that there is a need to review both this assumption and the assumption that the cation jump is the primary event in ion transport.

A tentative alternate approach to ion transport

We may reconsider in this context an important suggestion made in the literature by Greaves *et al.*[61], which has a direct bearing on transport but is not adequately discussed. This is the role of bond switching and consequent re-organization of NBOs in the glass structure. The role of NBO dynamics has also been considered by Elliott *et al.*[62], in understanding the near constant loss regime of frequency-dependent conductivities ($s \sim 1.0$). NBO–BO conversion leads to the formation of compositionally unexpected structural species in silicate glasses as observed in MAS NMR[63]. However, transport theories have paid little attention to the role of NBO–BO conversion. Bond switching is also an activated process and is presumably caused by thermal fluctuations. Therefore, the motion of NBOs may be considered as an inherently stochastic process. It is likely that NBO–BO excitations are involved in spacial movement of negative charge. The motion of NBOs from its immediate neighbourhood 'unsettles' an alkali ion in its site, which therefore is induced to follow suit. The 'hopping' NBO creates at the new place, a site equi-

valent to the one around which it was situated before switching. The 'unsettled' alkali ion will therefore move to the new equivalent position created by the hopping NBO. Therefore, it is possible to consider that NBO–BO bond-switching as the cause and the alkali transport as a consequence. Therefore, the primary step in ion transport may actually be the motion of NBO and not the migration of alkali ion from one site to another equivalent site in a structure, because NBOs are not likely to be positionally stay put on the timescale of alkali ion jump. The conductivities of mixed alkali glasses may therefore be examined from this point of view. The observed activation barriers in this approach actually represent the barrier for bond-switching or NBO migration and not the activation barriers for the individual cationic motions. The cation motions are secondary because they may not jump on their own from one site to an equivalent site, and the latter is strictly non-existent before NBO jumps occur. Several of the observations regarding MAE are reasonably, albeit qualitatively, well-accounted for using this approach.

(1) Since the primary step in conduction is bond-switching, the conductivity parameters refer to bond-switching and migration. Bond-switching requires the formation of an excited state – an intermediate state – where both BO and NBO are weakly coupled. This process, BO + NBO $\leftrightarrows$ BO·····NBO $\leftrightarrows$ NBO + BO, is associated with a local activation volume. We noticed earlier that in mixed alkali regions, the dissimilar alkali ions should be present in an optimal packing geometry in order to give rise to the observed density maximum and IR spectral features. The optimal packing, therefore, offers greater resistance to the formation of activated state in mixed alkali compositions compared to the single alkali situation and manifests as increase in activation barrier for bond-switching. This results as increased $E_{\text{d.c.}}$ in conductivity measurements. Optimal packing in a given mixed alkali composition is an average structural effect. Therefore, its influence on the activation energy for BO–NBO switching is also expected to be an average effect. All of the chemically similar bonds are affected to the same extent. This explains the observed Arrhenius behaviour and the single activation barrier in conductivity throughout the inter-alkali compositions.

(2) The observation of a single s in power law analysis of $\sigma_{\text{a.c.}}$ or single value of β in dielectric relaxation of the glasses implies that there is only one species or mode involved in a.c. response. This species or mode cannot be associated with alkalies because there are two of them, both of which should be active in middle compositions. In the present approach, this mode is associated with the dynamics of only the NBOs and the BO–NBO switching is a single mode. Thus the observed s or β behaviour is easily rationalized. Therefore, in the frequency regime in which measurements have been made, there is only one characteristic s or β and there is also minimum dispersion in their magnitudes. The present approach is not in disagreement with the observation of path selectivity in simulation studies[7,8,57–59]. This is because the alkali ion travels along a path charted out by the migrating NBOs. Further, at the new site of the migrating alkali ion, the environment may be equivalent to its earlier environment. Or, if that is not so, the unfavourable local energetics induces even more readily further migration of the NBO, which is then followed by the migration of the alkali ion. Thus the observed activation energy associated with the migration of the alkali ion is, in reality, the activation energy required for one or more NBO–BO switching operations as required for the destabilization of the alkali ion in its site.

This approach requires us to rationalize two more issues. Since the coordination numbers of Li^+ and Na^+ are different, does it entail a chosen pathway for the migration of NBOs. Indeed, this question is answered in the previous paragraph because NBO $\leftrightarrow$ BO switching itself is likely to exhibit such a preference. The initial and final positions of the NBO have to be similar if NBO has to stay in the new position long enough. Therefore, it has to be part of similar corner-sharing polyhedra. The availability of such equivalent polyhedra in the neighbourhood of the NBO may not constitute a problem. Secondly, since the present glass is a mixture of anionic species, we expect NBO $\leftrightarrow$ BO switching energies for the two glass-forming subsystems (TeO_2 and B_2O_3) to be different. Therefore, two distinct BO–NBO populations exist, which makes the situation indistinguishable from the two-alkali situation. However, this is not the case because it is not difficult to see that the destabilization of alkali sites may occur largely through BO–NBO switching of only the energetically weaker bond system. Further, if the two BO–NBO bond-switching energies are similar but not equal, simultaneous switching of both types of bonds occurs around an alkali ion site.

$$(\text{BO1} + \text{BO2}) + (\text{NBO1} + \text{NBO2}) \leftrightarrows (\text{NBO1} + \text{NBO2}) + (\text{BO1} + \text{BO2}).$$

Such coupled bond-switching not only restores the equality of initial and final states, but also ensures the presence of an average activation energy, which accounts for the observed single activation barrier. Perhaps in even more complex glasses constituted of different glass formers, metal–oxygen bonds of the network formers may possess significantly different ionicities. Also alkali ion coordination numbers may be different. In such a situation, distinct B–O populations will be present and give rise to distinguishable transport and relaxation behaviour. Indeed, presence of distinct M'' peaks as a consequence of such populations has been observed in mixed tri-alkali glasses[64].

(3) A satisfactory consequence of this approach is that it de-emphasizes the role of the masses of the alkali ions

about which contradictory observations[20,22,44,45] have been made, as noted earlier. Indeed, any mixed pair of cations can give rise to MAE, the incidence and magnitude of which has nothing to do with their masses, but more to do with their chemistry – polarizing power of the ions and electronegativities, which determines the strength of BOs. Presence of mixed ion effect similar to MAE in alkali–silver ion pair[65] and also alkali–alkaline earth ion pair[66] containing glasses is easily understandable from this model.

(4) The gradual disappearance of MAE at higher temperatures observed in most systems is a direct consequence of the loosening of the glass structure, which takes away the constraining influence of activation volume. It is also associated with increased dynamics of the BO ↔ NBO switching.

(5) Mixed anions with a single alkali can lead to increased conductivities in appropriate cases. It may be the consequence of either a reduction in the activation energy or increased BO ↔ NBO switching dynamics. Consider two anions, $[MO_{n/2}]^0$ ($\equiv A_1$) and $[M'O_{(m-1)/2}O]^-$ ($\equiv A_2$), which contain a BO and NBO respectively. The BO ↔ NBO switching between these two groups would lead to the formation of $[MO_{(n-1)/2}O]^-$ ($\equiv A_1'$)and $[M'O_{m/2}]^0$ ($\equiv A_2'$). From physical chemistry point of view, the switching is equivalent to a reaction $A_1 + A_2 \leftrightarrows A_1' + A_2'$. If electronegativities of A_1' and A_2' do not lie between those of A_1 and A_2, then one can expect an equilibrium where there is chemically-induced back and forth NBO–BO switching. This is a driving force for bond-switching in addition to thermal fluctuations. This increased BO ↔ NBO dynamics can lead to the observed increased alkali transport in mixed-anion glasses. When A_1–A_2 pairs are continuously connected in the structure, they may reduce the effective barrier by cooperatively accommodating the activation volume.

(6) The dielectric relaxation in glasses has been found almost universally to be governed by stretched relaxation function of the form $\phi(t) = \phi(0)\exp(-(t/\tau)^{\beta})$, where β is the stretching exponent and lies between 0 and 1. The origin of this universal behaviour indeed can be quantitatively accounted for[67] by considering the relaxation to be a two-step process in which polarization associated with an NBO after switching ($\phi_1(t)$) and polarization associated with the alkali ion ($\phi_2(t-t_0)$) relax independently and the two processes are separated by a time delay (t_0); $\phi(t) = \phi_1(t) + \phi_2(t-t_0)$.

Therefore, all experimental observations related to electrical transport in the present investigation and several observations which have been made with respect to mixed-alkali, mixed-cation and mixed-anion glasses in the literature appear to be consistent with the assumption that BO–NBO bond switching is the primary event in ion transport. It is necessary to add here that not every bond-switch operation needs be associated with a cation jump. It is enough even if a fraction of bond-switch operations creates necessary conditions for the alkali ion to follow suit. Although conductivity measurements are universally designed to measure parameters related to cation delivery at the cathode, in effect they all seem to measure anion transport. The measured activation barriers are the effective barriers for BO ↔ NBO bond-switching in all oxide-network-forming glasses. Indeed, the same consideration is applicable to the chalcogenide glasses, but the bond-switching in chalcogenides is more complex due to the existence of inter-chalcogen links.

Although the bond-switching event unseats an alkali ion in its neighbourhood, it is not implied that only isolated NBO–alkali ion pairs are present. Indeed, in glasses with significant degree of modification, it is easy to see that each alkali ion in the glass structure is actually surrounded by two or more shared NBOs. This requires a simultaneous switching of more than one NBO in the immediate neighbourhood of the alkali ion. In such situations it is implied that the observed activation barriers are a sum of the activation energies for that many BO ↔ NBO switchings in the neighbourhood of the alkali ion. Molecular dynamics studies[68] in lithium phosphate glasses have revealed that the Li^+ ions which jump most are those which are located in sites with a certain minimum number of NBOs (typically 2 and 3).

The question arises now as to how the Arrhenius expression is still valid for a bond-switching situation. In the expression,

$$\sigma = \sigma_0 \exp\left[-\frac{E_a}{kT}\right],$$

σ_0 represents 'infinite' temperature conductivity arising from alkali ion jumps. σ_0 is given by

$$\sigma_0 = \frac{n(Ze)^2\lambda^2\nu_0}{6kT}\exp\left(\frac{\Delta S_m}{k}\right).$$

The parameters may all be tentatively related to BO–NBO switching itself. ν_0 may be treated as the vibrational frequency of B–O bond, which undergoes stochastic excitation. λ is nearly the second neighbour distance because the switching occurs between neighbouring BO and NBO. $(Ze)^2$ is always unity as it relates to NBO and n, which is a concentration term, may be treated as the number of NBOs in the system. ΔS_m is an entropy term associated with the activation of BO. Thus σ_0 for the present situation may be written as,

$$\sigma_0 = \frac{aN\nu_0}{kT}\exp\left(\frac{\Delta S_m}{k}\right),$$

where a is of the order of unity which absorbs all other constants. The only assumption made is that the NBOs migrate instead of the alkali ions and that the Nernst–Einstein relation is valid for the migration of NBOs also. This approach helps us recover the Arrhenius equation with a new meaning. We may note that ν_0 for B–O vibra-

tions is of the same order of magnitude as that for the alkali ion vibration in its cage and the values are in the region of 10^3–10^2 cm^{-1}.

Conclusion

Mixed alkali boro-tellurite glasses are structurally complex and exhibit MAE in many properties in both borate-rich and tellurite-rich compositions. MAE can be related to structural and bonding features resulting from unique speciation in the glasses. Transport studies reveal that while there is MAE in d.c. conductivity, there is no signature of it in a.c. conductivity or dielectric relaxation. In order to understand our observations, alkali ion transport is tentatively considered as a driven secondary event, NBO migration through BO–NBO switching is treated as the motivating primary event. This tentative approach provides a reasonable explanation of the transport behaviour both in d.c. and a.c. regimes. The implications of the approach have been discussed.

1. Day, D. E., *J. Non-Cryst. Solids*, 1976, **21**, 343.
2. Isard, J. O., *J. Non-Cryst. Solids*, 1969, **1**, 235.
3. Rao, K. J., *Structural Chemistry of Glasses*, Elsevier, 2002.
4. Ingram, M. D., *Phys. Chem. Glasses*, 1987, **28**, 215.
5. Stevels, J. M., *Verres Refract.*, 1951, **5**, 4.
6. Mazurin, O. V., *Structure of Glass*, Consultants Bureau, New York, 1965, vol. 4, p. 5.
7. Balasubramanian, S. and Rao, K. J., *J. Phys. Chem.*, 1993, **97**, 8835.
8. Rao, K. J., Balasubramanian S. and Damodaran, K. V., *J. Solid State Chem.*, 1993, **106**, 174.
9. Hendrickson, J. R. and Bray, P. J., *Phys. Chem. Glasses*, 1972, **13**, 43.
10. Kone, A., Reggiani, J. C. and Souquet, J. L., *Solid State Ion.*, 1983, **9**, **10**, 709.
11. Uchino, T., Sakka, T., Ogata, Y. and Iwasaki, M., *J. Non-Cryst. Solids*, 1992, **146**, 26.
12. Balaya, P. and Sunandana, C. S., *J. Non-Cryst. Solids*, 1994, **175**, 51.
13. Komatsu, T. and Noguchi, T., *J. Am. Ceram. Soc.*, 1997, **80**, 1327.
14. Komatsu, T., Ike, R., Sato, R. and Matusita, K., *Phys. Chem. Glasses*, 1995, **36**, 216.
15. Tomozawa, M., *J. Non-Cryst. Solids*, 1993, **152**, 59.
16. Matusita, K., Watanabe, T., Kamiya, K. and Sakka, S., *Phys. Chem. Glasses*, 1980, **21**, 78.
17. Sharaf, N. A., Ahmed, A. A. and Abbas, A. F., *Phys. Chem. Glasses*, 1998, **39**, 76.
18. Ruller, J. and Shelby, J. E., *Phys. Chem. Glasses*, 1988, **29**, 209.
19. Kamitsos, E. I., Patsis, A. P. and Chryssikos, G. D., *Phys. Chem. Glasses*, 1991, **32**, 219.
20. Hendrickson, J. R. and Bray, P. J., *J. Chem. Phys.*, 1974, **61**, 2754.
21. Jain, H. and Peterson, N. L., *J. Am.Ceram. Soc.*, 1983, **66**, 174.
22. Jain, H., Downing, H. L. and Peterson, N. L., *J. Non-Cryst. Solids*, 1984, **64**, 335.
23. Rao, K. J. and Sundar, H. G. K., *Phys. Chem. Glasses*, 1980, **21**, 216.
24. Murthy, M. K. and Kirby, E. M., *Phys. Chem. Glasses*, 1964, **5**, 144.
25. Zhong, J. and Bray, P. J., *J. Non-Cryst. Solids*, 1989, **111**, 67.
26. Selvaraj, U. and Rao, K. J., *Spectrochim. Acta, Part A*, 1984, **40**, 1081.
27. Rao, K. J. and Bhat M. H., *Phys. Chem. Glasses*, 2001, **42**, 255.
28. Imaoka, M. and Yamazaki, T., *Yogyo Kyokai Shi*, 1968, **76**, 160.
29. Kamitsos, E. Z., Yiannopoulos, Y. D., Karakassides, M. A., Chryssikos, G. D. and Jain, H., *J. Phys. Chem.*, 1996, **100**, 11755.
30. Ito, K., Moynihan, C. T. and Angell, C. A., *Nature*, 1999, **398**, 492.
31. Rao, K. J., Kumar, S. and Bhat, M. H., *J. Phys. Chem. B*, 2001, **105**, 9024.
32. Himei, Y., Osaka, A., Nanba, T. and Miura, Y., *J. Non-Cryst. Solids*, 1994, **177**, 164.
33. Ilieva, D., Dimitrov, V., Dimitriev, Y., Bogachev, G. and Krastev, V., *Phys. Chem. Glasses*, 1998, **39**, 241.
34. Sekiya, T., Mochida, N., Ohtsuka, A. and Soejima, A., *J. Non-Cryst. Solids,* 1992, **151**, 222.
35. Tatsumisago, M., Minami, T., Kowada, Y. and Adachi, H., *Phys. Chem. Glasses*, 1994, **35**, 89.
36. Prabakar, S., Rao, K. J. and Rao, C. N. R., *Proc. R. Soc. London, Ser. A*, 1990, **429**, 1.
37. Jonscher, A. K., *Nature*, 1977, **267**, 673.
38. Almond, D. P., Duncan, G. K. and West, A. R., *Solid State Ion.*, 1983, **8**, 159.
39. Almond, D. P., Hunter, C. C. and West, A. R., *J. Mater. Sci.*, 1984, **19**, 3236.
40. Almond, D. P., West, A. R. and Grant, R. J., *Solid State Commun.*, 1982, **44**, 1277.
41. Macedo, P. B., Moynihan, C. T. and Bose, R., *Phys. Chem. Glasses*, 1972, **13**, 171.
42. Moynihan, C. T., Boesch, L. P. and Laberge, N. L., *Phys. Chem. Glasses*, 1973, **14**, 122.
43. Sanderson, R. T., *Polar Covalence*, Academic Press, 1983.
44. Angell, C. A., *Chem. Rev.*, 1990, **90**, 523
45. Jain, H. and Mundy, J. N., *J. Non-Cryst. Solids,* 1987, **91**, 315.
46. Elliott, S. R. and Henn, F. E. G., *J. Non-Cryst. Solids,* 1990, **116**, 179.
47. Elliott, S. R., *Adv. Phys.*,1987, **35**, 135.
48. Elliott, S. R., *Solid State Ion.*, 1988, **27**, 131.
49. Elliott, S. R., *Mater. Sci. Eng., B*, 1989, **3**, 69.
50. Rao, K. J., Estournes, C., Minetrier, M. and Levasseur, A., *Philos. Mag. B*, 1984, **70**, 809.
51. Rao, K. J., Estournes, C., Levasseur, A., Shastry, M. C. R. and Minetrier, M., *Philos. Mag. B.*, 1993, **67**, 389.
52. Rao K. J., Baskaran, N., Ramakrishnan, P. A., Ravi, B. G. and Karthikeyan, A., *Chem. Mater.*, 1998, **10**, 3109.
53. Verhoef, A. H. and den Hartog, H. W., *Solid State Ion.*, 1994, **68**, 305.
54. Chen, R., Yang, R., Durand, B., Pradel, A. and Ribes, M., *Solid State Ion.*, 1992, **53–56**, 1194.
55. Ngai, K. L., *J. Non-Cryst. Solids*, 1996, **203**, 232.
56. Ngai, K. L. and Martin, S. W., *Phys. Rev. B*, 1989, **40**, 10550.
57. Maas, P., Bunde, A. and Ingram, M. D., *Phys. Rev. Lett.*, 1992, **68**, 3064.
58. Kirchheim, R. and Paulmann, D., *J. Non-Cryst. Solids*, 2001, **286**, 210.
59. Montani R. A., *J. Non-Cryst. Solids*, 1997, **215**, 307.
60. Sunandana, C. S., *Bull. Mater. Sci.*, 1995, **18**, 17.
61. Greaves, G. N., Gurman, S. J., Catlow, C. R. A., Chadwick, A. V., Houde-Walter, S., Henderson, C. M. B. and Dobson, D. B., *Philos. Mag. A*, 1991, **69**, 1059.
62. Elliott, S. R., *J. Non-Cryst. Solids*, 1994, **170**, 97.
63. Rao, C. N. R., Thomas, J. M., Klinowski, J., Selvaraj, U., Rao, K. J., Millward, G. R. and Ramdas, S., *Angew. Chem.*, 1985, **24**, 61.
64. Rao, K. J. and Kumar, S., *Curr. Sci.*, 2003, **85**, 945.
65. Chowdari, B. V. R. and Radhakrishnan, K., *Solid State Ionics*, 1987, **23**, 81.
66. Shelby, J. E., *J. Non-Cryst. Solids*, 2000, **263** & **264**, 271.
67. Kumar, S. and Rao, K. J., *Chem. Phys. Lett.*, 2004, **387**, 91.
68. Karthikeyan, A., Vinatier, P., Levassuer, A. and Rao, K J., *J. Phys. Chem.*, 1999, **103**, 6185.

Received 31 January 2004; accepted 4 February 2004